# Molecular Ionization of Cyclohexanone in Femtosecond Laser Fields: An Application of ADK Theory[1]

**Q. Q. Wang[a], H. Mineo[b], D. Wu[a], M. X. Jin[a], C. H. Chin[c], Y. Teranishi[d], S. D. Chao[b], D. Ding[a], *, and S. H. Lin[d, e]**

[a] Institute to Atomic and Molecular Physics, Jilin University, Changchun, 130012 China
[b] Institute of Applied Mechanics, National Taiwan University, Taipei 106, Taiwan
[c] National Synchrotron Radiation Research Center, Hsinchu 30076, Taiwan
[d] Department of Applied Chemistry, National Chiao-Tung University, Hsin-Chu 300, Taiwan
[e] Institute of Atomic and Molecular Sciences, Academia Sinica, Taipei 106, Taiwan
*e-mail: dajund@jlu.edu.cn
Received March 10, 2009

**Abstract**—The mechanisms of ionization and dissociation of cyclohexanone ($C_6H_{10}O$) in a 90 fs, 788 nm linearly polarized laser field ranging from $10^{13}$ to $10^{14}$ W/cm$^2$ by a time-of-flight mass spectrometer (TOF-MS) have been investigated. The ion yields as a function of laser intensity have been measured experimentally. By comparison with the Ammosov–Delone–Krainov (ADK) theory based on a hydrogen-like model, the ionization mechanism of cyclohexanone in this intense femtosecond laser field has been understood. Considering the importance of molecular nuclear motions, we propose that the Franck–Condon (F–C) factor can provide the excess vibrational energy in the molecular ion. This energy is required for the decomposition of the molecular ion which finally results in the observed mass spectrum.
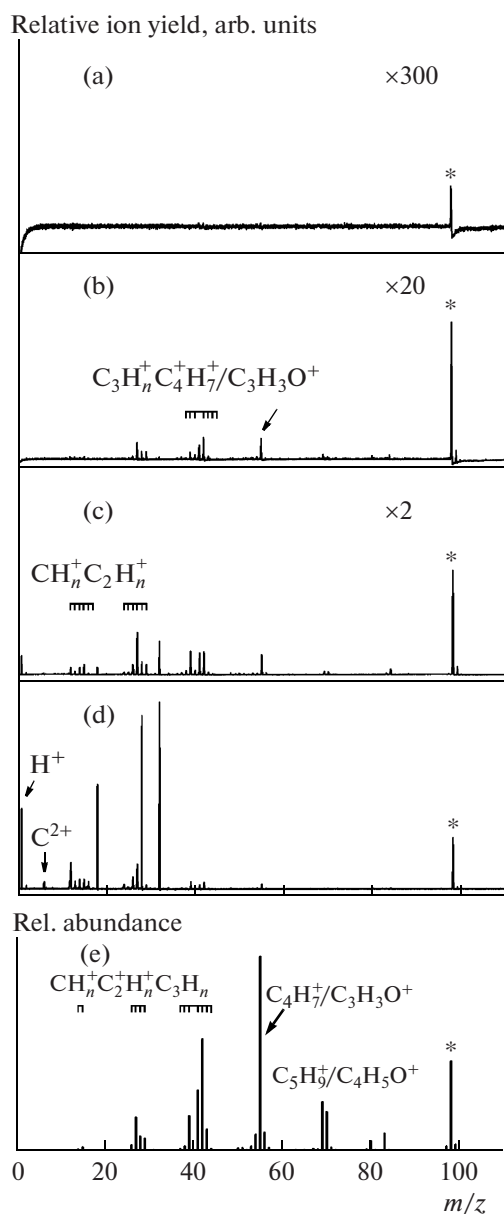
## 1. INTRODUCTION

The behaviors of atoms and molecules in intense femtosecond (fs) laser field are of interesting domain with the advent of the femtosecond laser [1, 2]. Many phenomena have been explored such as molecular alignment [3], high harmonic generation [4] and so on, which are related to the basic interaction of laser field with atoms and molecules. Actually, as the most common phenomenon, ionization of atoms has been widely investigated for almost fifty years or even longer. In 1964, Keldysh [5] derived the expressions for the ionization probability of atoms in the field whose strength is compared to the atomic field strength. A famous parameter, adiabatic parameter (also named Keldysh parameter) was proposed to determine the boundary between multiphoton ionization and tunneling ionization. Another popular atomic tunneling ionization theory was proposed by Faisal [6] based on the Keldysh theory and developed with the S-matrix formalism by Reiss [7] (KFR theory). Due to the complexity of the formula provided by Keldysh or KFR theory, it is necessary to develop simpler ones for common use especially for tunneling region. Perelomov et al. [8] suggested a simple model to calculate the ionization probability from an arbitrary state of a hydrogen atom in an alternating electric

field, and this model was named the Perelomov–Popov–Terent'ev (PPT) theory. In order to extend this simple formula model to arbitrary atoms in arbitrary states, Ammosov, Delone, and Krainov have extended the PPT theory by introducing the effective principle orbital quantum number (usually called ADK theory) [9]. The influence of the polarization was also mentioned in their work. It should be noticed that the phenomena of most rare gas atoms (Xe, Kr and Ar) in the higher laser intensity range were predicted well by ADK theory [10]. However, the theories mentioned above are all for treating atoms originally. Considering the characteristics of the molecules, ionization probabilities for molecules are more complicated to calculate, especially for polyatomic molecules. Chin et al. showed well agreements between the predicted ionization rates of some simple molecules ($H_2$, $O_2$, $N_2$, CO, NO and $CO_2$) by ADK theory and the experimental observations [11]. Subsequently, some experimental studies of molecules in intense laser field exhibited strong suppressions by comparing the diatomic molecules with their companion atoms, for example, $O_2$ and Xe (ionization energy of 12.07 and 12.13 eV, respectively). In order to interpret these suppression phenomena, Tong et al. developed the ADK theory by considering the difference in the electronic wave functions between atoms and molecules (referred to MO-ADK theory) [12]. On the other hand, by combining

---

[1] The article is published in the original.

Relative ion yield, arb. units

(a)    ×300

(b)    ×20

$C_3H_n^+ C_4H_7^+/C_3H_3O^+$

(c)    ×2

$CH_n^+ C_2H_n^+$

(d)

$H^+$

$C^{2+}$

Rel. abundance

(e)

$CH_n^+ C_2H_n^+ C_3H_n$    $C_4H_7^+/C_3H_3O^+$

$C_5H_9^+/C_4H_5O^+$

0    20    40    60    80    100

*m/z*

**Fig. 1.** Mass spectra of cyclohexanone interacted with 90 fs laser pulses at 788 nm for four different intensities: (a) $3.6 \times 10^{13}$; (b) $6.8 \times 10^{13}$; (c) $1.6 \times 10^{14}$; (d) $4.1 \times 10^{14}$ W/cm$^2$. The mass spectrum obtained by EI method is also listed in (e) [19]. The asterisk denotes the parent ion.

the molecular orbital (MO) theory and the Born-Oppenheimer (BO) approximation, Lin and his co-workers proposed the generalized Keldysh (g-Keldysh) [13] and KFR (g-KFR) theory [14], which were proved to be suitable for treating polyatomic molecules (methane, cyclopentanone, et al.) experimentally [15, 16].

In this work, we shall apply the ADK theory combined with the characteristics of the $2p$-orbital for the ionization process of cyclohexanone in intense fs laser field. The quantitative calculated results are compared

with the experimental observations. Although the ADK theory overestimates the ionization rate of cyclohexanone in intense fs laser field, it can predict the saturation intensity well. Moreover, we propose that the F–C factor, which is calculated on the basis of the ionization rate provided by molecular ADK theory, may exhibit the probability distribution of the excess energy in the ions by ionization. It is regarded to be important for interpreting further decomposition of the molecular ions.

## 2. EXPERIMENTAL DETAILS

The experimental apparatus used for the fs laser ionization/dissociation study has been described elsewhere [16–18]. Briefly, a chirped pulse amplified (CPA) Ti:sapphire laser (TSA, Spectra-Physics) was employed, which produced a 90 fs, linearly polarized laser beam with a repetition rate of 10 Hz and a wavelength centered at 788 nm. The laser intensity was varied using a rotatable half-wave plate followed by a Glan–Taylor prism, which can also ensure that the direction of laser polarization is parallel or perpendicular to the flight axis of the mass spectrometer always during changing the beam intensity. The laser beam was focused by a quartz plano-convex lens ($f = 350$ mm) onto the molecular beam, providing laser intensities in the range of $10^{13}$ to $10^{14}$ W/cm$^2$. The molecular beam was generated by a pulsed valve with 400 μs duration in a vacuum chamber with a background pressure of $10^{-5}$ Pa and commercial cyclohexanone sample (Aldrich Co. Ltd., 99% purity) was used without further purification. A linear TOF-MS was operated on Wiley-McLaren focusing condition. The produced ions were introduced into a 90 cm field-free region after two-step acceleration and finally were detected by a dual microchannel plate detector. A slit with 0.5 mm width was mounted in front of the flight tube for ensuring that only the ions produced in the center portion of the laser focus volume can enter the drift tube. The width of the slit was chosen not larger than the Rayleigh length. By connecting the ion detector output through a fast preamplifier to a digital storage oscilloscope (Tektronix TDS 3054B), mass spectra were accumulated and averaged over 512 laser shots normally and then transferred into a computer. Typically the mass resolution was $m/\Delta m = 1000$ at $m/e = 100$. Ion intensities (corresponding to ion yields) were evaluated by integrating the ion signals.

## 3. RESULTS

The TOF mass spectra of cyclohexanone at the intensities of $3.6 \times 10^{13}$, $6.8 \times 10^{13}$, $1.6 \times 10^{14}$, and $4.1 \times 10^{14}$ W/cm$^2$ are shown in Figs. 1a–1d, respectively. The singly-charged parent ion represented by the asterisk is dominant in the mass spectra at low intensity, with very little fragmentation (Fig. 1a). With increasing the laser intensity, some large fragment ions
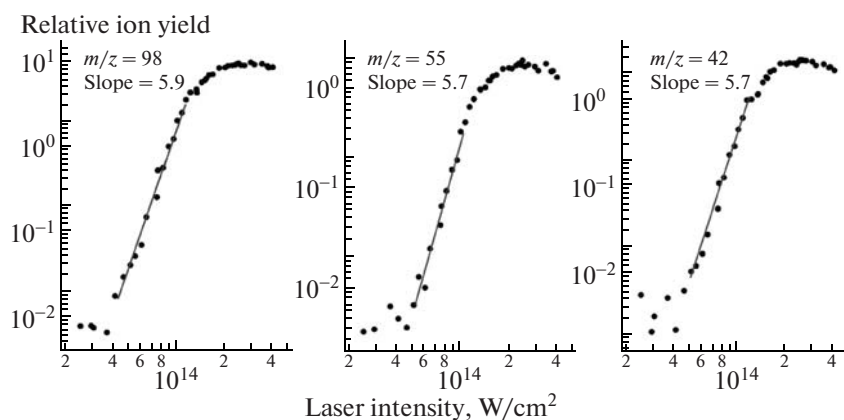
Relative ion yield



**Fig. 2.** Relative ion yields of parent and main fragment ions as a function of laser intensity. The laser wavelength is 788 nm. A linear fit through the data points is shown as the solid line.

appear though the singly-charged parent ion is still predominant. But the extensive fragmentation is observed at high laser intensity, being accompanied by weak doubly-charged carbon ion ($C^{2+}$). Hydrogen ion also appears in the intensity region higher than $1 \times 10^{14}$ W/cm$^2$ and increases rapidly with increasing laser intensity. From all mass spectra, the singly-charged parent ion is clearly seen while only small evidence for the existences of the doubly- and multiply-charged parent ions are observed because the dissociation of molecular ions or any other processes may occur.

Experimentally, the fragment ion is assigned to $CH_3$-loss molecular ion with $m/z = 83$ in Fig. 1. The other fragment ions are also identified as follows: series of $C_4H_n^+$ ($n = 0$–$8$), $C_3H_n^+$ ($n = 0$–$7$), $C_2H_n^+$ ($n = 0$–$5$), $CH_n^+$ ($n = 0$–$3$), $C^{2+}$, $H_2^+$, and $H^+$. Moreover, some peaks should be paid more attention: by taking into account of the similar molecular structures between cyclohexanone and cyclopentanone, on the basis of the dissociation patterns of the cyclopentanone ions [16], the fragment ions with $m/z = 56$ or 55 may also be designated to $C_3H_4O^+$ or $C_3H_3O^+$, respectively, which are the primary dissociation products of $C_6H_{10}O^+$. Furthermore, the peaks located at $m/z = 32$ and 18 are more likely to be $O_2^+$ and $H_2O^+$ from the residual gas in vacuum.

Simultaneously, in this work the mass spectra obtained by the femtosecond ionization are also compared with that provided by electron impact (EI) method, seen in Fig. 1e [19]. The peak positions of two kinds of mass spectra are identical but the relative peak abundances are differed. On the one hand, the EI mass spectrum illustrates a clear parent ion accompanied by heavy fragmentation. The fragment ion with $m/z = 55$ is predominant in mass spectrum. On the contrary, femtosecond ionization shows a great deal of information being obtained by various intensities. One of the most important observations is that the mass spectrum

shows a pattern of intact parent ion with few fragment ions at low laser intensities, which could be employed for the identification of molecules. On the other hand, the small fragment ions with $m/z$ smaller than 20 cannot be obtained by EI method but those small fragment ions, even hydrogen ion could be observed at high intensities for most of hydrocarbon molecules [15] by femtosecond ionization. We suggest that the variations of the available internal energy obtained by different methods may lead to the differences in the rate constants for dissociation of the ions, which induce the different dissociation patterns. Femtosecond ionization-dissociation mechanism induces a heavy fragmentation, implying that in this experimental condition cyclohexanone parent ion possesses more available internal energy than in EI method.

## 4. DISCUSSION

We take a simple estimation for our experimental conditions following a Keldysh parameter ($\gamma$) calculation based on atomic-like model. In present work, the obtained value of $\gamma$ tends to 1 when laser intensity is around $8 \times 10^{13}$ W/cm$^2$, suggesting that the multiphoton ionization mechanism should be taken into consideration below this intensity as the most of cases in our experiment.

The ion yields of the parent ion and two fragment ions, $m/z = 55$ and 42, as a function of the laser intensity are shown in Fig. 2 in a log-log plot. The laser dependence of the parent ion shows a slope of 5.9 by measuring its ion peak area in the mass spectrum, which is closed to the minima photon number required for ionizing this molecule as the ionization potential of cyclohexanone is 9.16 eV. From Fig. 2 we find that $m/z = 55$ and 42 peaks exhibit a photon number of 5.7, which are also closed to 6, implying that these two fragment ions may be primarily dissociated from the parent ion. This result suggests that the multiphoton ionization mechanism may play an impor-

Relative Ion yield
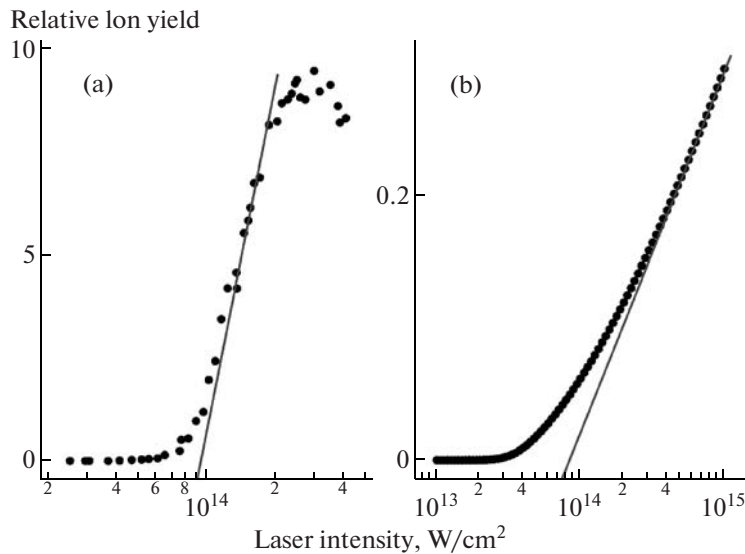


**Fig. 3.** Ion yields as a function of laser intensity on a semi-log plot. (a) The saturation intensity of cyclohexanone in fs laser field is $9.0 \times 10^{13}$ W/cm$^2$; (b) The saturation intensity of cyclohexanone predicted by ADK theory is $7.5 \times 10^{13}$ W/cm$^2$.

tant role under our experimental conditions, which is coincident with the prediction of Keldysh parameter and is also consistent with our previous study of cyclopentanone [16].

In order to further investigate the ionization process, we quantitatively calculate the ionization rate of cyclohexanone in intense laser field by ADK theory [9] based on a hydrogen-like atom approach. The probability of ionization is described by [20]

$$w = \left(\frac{3e}{\pi}\right)^{3/2} \frac{Z^2}{3n^{*3}} \frac{2l+1}{2n^*-1} \left[\frac{4eZ^3}{(2n^*-1)n^{*3}F}\right]^{2n^*-3/2} \times \exp\left[\frac{-2Z^3}{3n^{*3}F}\right], \quad (1)$$

where $l$ is the orbital quantum number, $Z$ is the ionic charge, $F$ is the electric field strength of the laser, and $n^*$ is the effective quantum number which can also be expressed as

$$n^* = \frac{Z}{\sqrt{2E_0}}, \quad (2)$$

with $E_0$ is the ionization potential.

Considering the molecular structure of cyclohexanone, the highest occupied molecular orbitals (HOMO) is a non-bonding orbital of the C–O group, which has the $p$-orbital character. The HOMO and geometry optimizations are performed by ab initio quantum chemical calculation. The B3LYP/6-31G** method [21, 22] has been used to carry out geometry optimization and the energy of the ion has been refined by the G3(MP2,CCSD) ab initio calculation [23, 24]. The zero-point energy correction to the total G3(MP2,CCSD) energy has been computed using

B3LYP/6-31G** frequency. All ab initio calculations have been performed using the GAUSSIAN 03 package [25]. The calculated ionization potential energy of cyclohexanone is 9.18 eV, which is closed to the experimental measurements [19]. The results illustrate that the HOMO of cyclohexanone is mainly consisted of the 2$p$-atomic orbitals (AOs). Therefore, we choose one of 2$pz$ AOs with the ionization potential energy 9.18 eV in calculating the ionization rate. In addition, by taking into account time and spatial distribution of the laser pulses, we define the spatial averaged ionization yield as

$$\overline{M^{i+}(t)} = 4\pi \int_0^\infty dR R^2 M^{i+}(t, R). \quad (3)$$

One of the most significant contributions of the ADK theory is to predict the saturation intensity, especially for rare gas and diatomic molecules. The calculated result was fitted very well with the experimental measurement of tunnel ionization of Xe atom by Chin and his co-workers [11]. This result is popular up to the present and is always applied to scale the laser intensity. In Fig. 3, the yields are plotted as a function of laser intensity on a semi-log plot, and the saturation intensity is estimated from the extrapolated line as the crossing point with the logarithmic laser intensity axis [26]. It should be noticed that the saturation intensity obtained by the experimental observation is $9 \times 10^{13}$ W/cm$^2$ approximately, which is larger than that estimated by ADK calculation within a factor of 1.2.

Moreover, the photoionization rate constants of cyclohexanone and its cation as a function of laser intensity are illustrated in Fig. 4a. The ADK theory overestimates the rate constants for higher intensity,
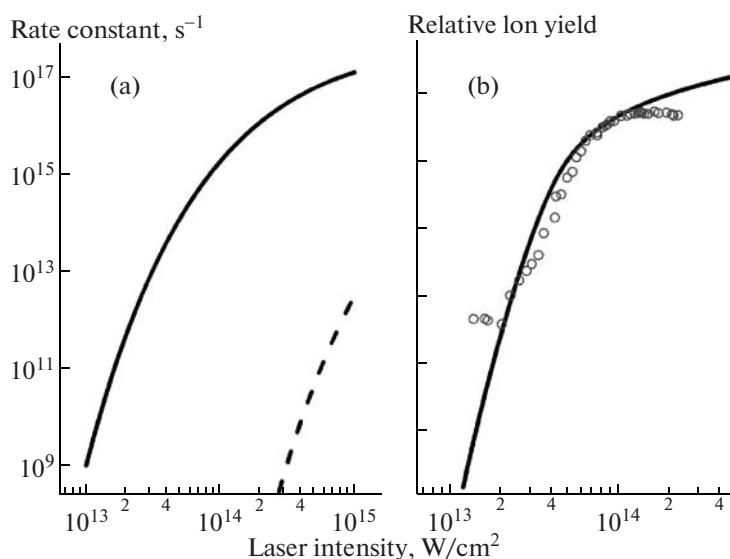
**Fig. 4.** Calculation results for the first (and the second) ionization rate constant of cyclohexanone by predicting of ADK theory (a); Comparison of relative ion yields between experimental and theoretical results (b).

especially for the intensity above $10^{15}$ W/cm$^2$ where the values of the rate constants go beyond $10^{17}$ s$^{-1}$. In Fig. 4a, it is notable that the rate constants for the second ionization are much smaller than that for the first ionization, differed by a factor $10^4$ at even $10^{15}$ W/cm$^2$. This result may be used to understand the reason that the doubly-charged cyclohexanone parent ions are not observed in all mass spectra.

By comparison of the theoretical and experimental results as shown in Fig. 4b, some overestimates of the rate constants result in a relatively higher ion yield of singly-charged cyclohexanone ion predicted by the theory in the range below the saturation intensity. At the higher laser intensities above the saturation intensity, a departure from the predicted curve is observed. It should be noticed that the contribution of the dissociation processes may become more and more significant for higher laser intensity, while the ADK theory ignores the influence of the fragmentation. In addition, the absence of the laser frequency in formula (1) may also be considered. Therefore, it is reasonable to observe a deviation between experimental measurement and ADK theory prediction in this high intensity region.

It is worth noting that up to the present only the electronic motion in the ionization has been discussed actively. The nuclear motions, which are the characteristics of molecules, should be also considered [27]. In this situation, by taking into account of the initial and final vibrational states, we propose that the rate constant for the molecular ion at a vibrational state should be expressed by the product of the F–C factor and the rate constant calculated by the molecular ADK theory. And then the probability distribution of the excess vibrational energy in the molecular ion can

be obtained. It is important to have the knowledge of this excess vibrational energy required for the decomposition of the molecular ion which finally results in the observed mass spectrum.

At last, we attempt to explain the dissociation pattern of cyclohexanone induced by intense fs laser field on the basis of the understanding of cyclopentanone whose structure is similar to cyclohexanone. In our previous study [16, 18, 28], we pointed out that the ionization followed by dissociation may be the main process when the fs laser interacted with cyclopentanone since for neutral dissociation of a molecule to take place, the molecule has to absorb energy from the laser first and then the molecule will either predissociate or decompose after internal conversion; the decomposed products then ionize afterwards, and all these steps have to take place within the laser pulse duration of ~100 fs. This explanation may also be used in cyclohexanone case. Furthermore, the $m/z = 56$ peak may be assigned to the $C_4H_8^+$ or $C_3H_4O^+$ while the peaks at $m/z = 55$, 28, and 27 can be explained by secondary dissociation processes, and the $H^+$ observed at high intensity is probably originated from the elimination of $H^+$ of dications. Nevertheless, it should be mentioned that the laser field will also modified the potential energy surfaces of cyclohexanone molecule (or molecular ions) if electric field strength is intense enough. Therefore, this kind of dissociation channel, such as field-assisted dissociation et al., should also be considered in intense laser-induced dissociation processes.

## 5. CONCLUSIONS

In this work we study the ionization and dissociation processes of cyclohexanone by 90 fs intense laser field at 788 nm, ranging from $2 \times 10^{13}$ to $4 \times 10^{14}$ W/cm$^2$. The ionization followed by dissociation reaction channel is recognized to be the main process. The observed laser dependence of the cyclohexanone parent ion shows a consistency with the minimum photon number ionization needs. By combining this result and the prediction of the Keldysh parameter, it is reasonable to believe that multiphoton ionization plays an important role if laser intensity is lower than the saturation intensity ($8 \times 10^{13}$ W/cm$^2$).

The quantitative calculations of the ionization rates for cyclohexanone molecule and its cation are carried out by using ADK theory based on the hydrogen-like model. The prediction of the saturation intensity by ADK theory is seen to fit well with the experimental measured one within a factor of 1.2. Unfortunately, an obvious deviation of the ion yield is seen at high intensity, which may due to the influence of the fragmentation or the neglect of the laser frequency.

Moreover, considering the vibration characteristics of the molecules, we propose that the probability distribution of the excess energy would be obtained by calculating the F–C factor involved in the ionization process. It is considered to be a more effective method which could provide important information for further theoretical interpreting of these molecular ions decomposition, i.e., the Rice–Ramsperger–Kassel–Marcus (RRKM) calculations of dissociation of the ions.

## ACKNOWLEDGEMENTS

## REFERENCES

1. S. M. Hankin, D. M. Villeneuve, P. B. Corkum, et al., Phys. Rev. Lett. **84**, 5082 (2000).
2. S. L. Chin, *Advances in Multi-photon Processes and Spectroscopy* (World Sci., Singapore, 2004).
3. S. Kaziannis, C. Kosmidis, and A. Lyras, J. Phys. Chem. A **112**, 4754 (2008).
4. X. Zhou, X. M. Tong, Z. X. Zhao, et al., Phys. Rev. A **72**, 033412 (2005).
5. L. V. Keldysh, Sov. Phys. JETP **20**, 1307 (1965).
6. F. H. M. Faisal, J. Phys. B: At. Mol. Phys. **6**, L89 (1973).
7. H. R. Reiss, Phys. Rev. A **22**, 1786 (1980).
8. A. M. Perelomov, V. S. Popov, and M. V. Terent'ev, Sov. Phys. JETP **23**, 924 (1966).
9. M. V. Ammosov, N. B. Delone, and V. P. Krainov, Sov. Phys. JETP **64**, 1191 (1986).
10. S. L. Chin, F. Yergeau, and P. Lavigne, J. Phys. B: At. Mol. Phys. **18**, L213 (1985).
11. T. D. G. Walsh, F. A. Ilkov, J. E. Decker, et al., J. Phys. B: At. Mol. Phys. **27**, 3767 (1994).
12. X. M. Tong, Z. X. Zhao, and C. D. Lin, Phys. Rev. A **66**, 033402 (2002).
13. K. Mishima, M. Hayashi, J. Yi, et al., Phys. Rev. A **66**, 033401 (2002).
14. H. Mineo, S. D. Chao, K. Nagaya, et al., Chem. Phys. Lett. **439**, 224 (2007).
15. M. Sharifi, F. Kong, S. L. Chin, et al., J. Phys. Chem. A **111**, 9405 (2007).
16. Q. Q. Wang, D. Wu, M. X. Jin, et al., J. Chem. Phys. **129**, 204302 (2008).
17. D. Wu, Q. Q. Wang, X. H. Cheng, et al., J. Phys. Chem. A **111**, 9494 (2007).
18. Q. Q. Wang, D. Wu, D. D. Zhang, et al., J. Phys. Chem. C (2009, in press).
19. *Mass Spectra in NIST Chemistry WebBook*, Ed. by P. J. Linstrom and W. G. Mallard (NIST Standard Ref. Database Nat. Inst. Stand. Technol., Gaithersburg, MD, 2005), Vol. 69.
20. F. A. Ilkov, J. E. Decker, and S. L. Chin, J. Phys. B: At. Mol. Phys. **25**, 4005 (1992).
21. A. D. Becke, J. Chem. Phys. **98**, 5648 (1993).
22. C. Lee, W. Yang, and R. G. Parr, Phys. Rev. B **37**, 785 (1988).
23. A. G. Baboul, L. A. Curtiss, P. C. Redfern, et al., J. Chem. Phys. **110**, 7650 (1999).
24. L. A. Curtiss, K. Raghavachari, P. C. Redfern, et al., Chem. Phys. Lett. **314**, 101 (1999).
25. M. J. Frisch, G. W. Trucks, H. B. Schlegel, et al., *Gaussian 03, Revision B.4* (Gaussian Inc., Pittsburgh, 2003).
26. S. M. Hankin, D. M. Villeneuve, P. B. Corkum, et al., Phys. Rev. A **64**, 013405 (2001).
27. K. Mishima, K. Nagaya, M. Hayashi, et al., *Advances in Multi-photon Processes and Spectroscopy* (World Sci., Singapore, 2006).
28. Y. Teranishi, M. Hayashi, F. Kong, et al., Mol. Phys. **106**, 333 (2008).